Published in final edited form as:
Cancer. 2008 November 15; 113(10): 2779–2789. doi:10.1002/cncr.23899.

Epithelial and Pseudoepithelial Differentiation in Glioblastoma and Gliosarcoma: A Comparative Morphologic and Molecular Genetic Study

Fausto J. Rodriguez, M.D.[1], **Bernd W. Scheithauer, M.D.**[1], **Caterina Giannini, M.D., PhD.**[1], **Sandra C. Bryant, M.S.**[2], and **Robert B. Jenkins, M.D., PhD.**[1]

[1]Department of Laboratory Medicine and Pathology, Division of Biostatistics, Mayo Clinic College of Medicine, Rochester, MN, United States

[2]Department of Health Sciences Research, Division of Biostatistics, Mayo Clinic College of Medicine, Rochester, MN, United States

Abstract

Background—Glioblastomas exhibit a remarkable tendency to morphologic diversity. Although rare, pseudoepithelial components (adenoid or epithelioid) or true epithelial differentiation may occur and poses a significant diagnostic challenge.

Methods—H&E slides were reviewed and immunohistochemistry and fluorescence in situ hybridization were performed.

Results—The patients included 38 males and 20 females. Median age at diagnosis was 57 years (IQR, 50 to 67), and median overall survival was 7 months (IQR, 4 to 11). “Adenoid” glioblastomas (A-GBM) predominated (48%). True epithelial glioblastomas (TE-GBM) were next most frequent based on morphology and immunohistochemistry (35%), followed by epithelioid glioblastomas (E-GBM) (17%). Overall 25 (43%) tumors featured a sarcomatous component. Molecular cytogenetic abnormalities identified by FISH in A-GBM, EGBM and TE-GBM respectively included *p16* deletion/-9 (60%, 71%, 64%); chromosome 10 loss (40%, 63%, 57%), chromosome 7 gain without *EGFR* amplification (70%, 38%, 40%), *EGFR* amplification (10%, 50%, 27%), *PTEN* deletion (10%, 25%,29%), *PDGFRA* amplification (10%, 25%, 0%), and *RB1* deletion/-13q (50%, 0%, 14%). Abnormalities identified by IHC included p21 immunonegativity (60%, 25%, 93%), that was most frequent in TE-GBM (p=0.008), strong diffuse p53 staining (29%, 29%, 41%), strong membranous staining for EGFR (21%, 63%, 19%) most frequent in E-GBM (p=0.03), and an increased frequency of p27 immunonegativity in gliosarcomas (15% negative, 85% focal) compared to tumors without sarcoma (38% strongly positive)(p=0.009).

Conclusion—Pseudoepithelial and true epithelial morphology are rare phenomena in GBM and may be associated with a similar poor prognosis. These tumors demonstrate proportions of molecular genetic abnormalities varying somewhat from conventional GBM.

Keywords

glioma; glioblastoma; brain; epithelial; adenoid; epithelioid; FISH

Correspondence to: Fausto J. Rodriguez.

Address Correspondence to: Fausto J. Rodriguez M.D. Mayo Clinic College of Medicine 200 First Street SW Mayo Clinic Rochester, MN 55905 Phone: (507) 538 9774 Fax: (507) 284 1599 e-mail: rodriguez.fausto@mayo.edu.

Introduction

Glioblastoma is the highest grade tumor in the spectrum of diffusely infiltrating astrocytic neoplasms. Remarkable in its morphologic diversity, various subtypes are recognized including fibrillary, the most common, as well as gemistocytic, giant cell, small cell and granular cell forms (1). When a sarcomatous element is evident the term gliosarcoma is applied. The sarcomatous component usually takes the form of fibrosarcoma or pleomorphic spindle cell sarcoma. Cartilaginous(2), osseous(3), skeletal(4) or smooth muscle(5) as well as adipocytic differentiation(6) have also been described.

A very uncommon morphologic variation in high grade astrocytomas is pseudoepithelial morphology. This consists most often of an “adenoid” pattern mimicking adenocarcinoma(7-10), and less frequently simply a large cell or “epithelioid” pattern(11,12). True epithelial differentiation in the form of squamous nests and true glands is a very rare occurrence(13-15).

The purpose of our current study is to delineate the morphologic and immunophenotypic features of glioblastomas with various degrees of epithelial appearance to further clarify the terminology, as well as to explore various molecular abnormalities in the largest series to date of such unusual tumors.

Materials and Methods

All studies were approved by the institutional review board. Cases were derived largely from the consultation files of one of us (BWS). In addition, the Mayo Clinic Tissue Registry was searched for glioblastomas with adenoid, epithelioid or true epithelial features accessioned from 1986 to 2007.

Criteria for Classification

All tumors were assigned to one of the three categories: adenoid glioblastoma (A-GBM), epithelioid glioblastoma (E-GBM), and glioblastoma with true epithelial differentiation (TE-GBM). Criteria for adenoid glioblastoma included the presence of cohesive cells of intermediate size compactly arranged in cords or nests, occasionally with pseudoglandular/cribriform spaces, but lacking immunohistochemical evidence of epithelial differentiation using tissue specific markers, such as low molecular weight cytokeratin (CAM5.2) and/or polyclonal carcinoembryonic antigen (pCEA). The identification of true epithelial differentiation required a morphologic epithelial appearance, including nests of cells with more generous cytoplasm than typically seen in adenoid examples, squamoid nests or true glandular structures, plus immunohistochemical expression of one or more of the above noted specific epithelial markers. In both the A-GBM and TE-GBM the respective diagnostic features were present in at least one low power field for inclusion of the case in the study. Epithelioid glioblastomas were 40-50% composed of large often round, process-poor cells with abundant cytoplasm and defined cell borders, but lacking immunoreactivity for epithelial specific markers.

Tissue Microarray

A tissue microarray was constructed using 29 cases for which adequately preserved tissue of appropriate thickness was available in paraffin blocks. At least three cores (0.6 mm in diameter each) per case were selected from various tissue components of the tumor representing A-GBM, E-GBM and TE-GBM. Non-neoplastic controls included human cerebral gray matter and white matter resected for chronic seizures, placenta, liver, and tonsil.

Immunohistochemistry

Employing a Dako autostainer and the Dual Link Envision+ detection system, immunohistochemical studies were performed upon 5μ formalin-fixed, paraffin-embedded sections using antibodies directed against glial fibrillary acidic protein (GFAP) (Dako, Carpinteria, CA, polyclonal; 1:4000), S100 protein (Dako, polyclonal; 1:1600), epithelial membrane antigen (EMA)(Dako, clone E29; 1:20), cytokeratin CAM 5.2 (Becton Dickinson, 1:50), cytokeratin AE1/AE3 (Zymed, South San Francisco, CA; 1:200), cytokeratin 5/6 (Zymed, D516B4; 1:200), cytokeratin 7 (Dako, OB-TL12/30; 1:200), cytokeratin 20 (Dako, Ks20.8; 1:50), CEA (Dako, polyclonal; 1:2000), TTF1 (Dako, 8G7G3/1; 1:1000), CDX2 (Novocastra, AMT28; 1:100), chromogranin (Chemicon; LK2H10; 1:500), synaptophysin (ICN, clone SY38; 1:40), neurofilament protein(Dako, clone 2F11, 1:75), INI-1-BAF47(BD transduction, clone 25;1:100), smooth muscle actin (SMA) (Dako, clone 1A4; 1:150), desmin (Dako, clone DER11; 1:100) ki67 (Dako, clone MIB-1, monoclonal; 1:300). MIB-1 labeling indices were evaluated in morphologically different tumor components using the CAS200 imaging system (Bacus Laboratories, Lombard, IL) and examining 20 consecutive fields.

Immunohistochemical studies using antibodies for p16 (NeoMarkers, clone16P07;1:400), p21 (Dako,SX118;1:25), p27/KIP-1 (Dako, SX53G8;1:100), p53 (Dako, clone DO7;1:2000), β-catenin (Santa Cruz, 1:200), E-cadherin (Zymed, clone 4A2C7; 1:2000), and epidermal growth factor receptor (EGFR)(Dako, 2-18C9; prediluted) were performed on TMA slides.

Immunohistochemical Scoring

Immunohistochemical markers were scored in the glial and adenoid/epithelial component when feasible. If only one component was represented in the slide then that component was evaluated exclusively. For EGFR, p16,p21,p27,p53 and beta catenin, the median of several (at least 3) measurements was used for correlative analyses. Since true epithelial differentiation was often limited to small areas, focal but clear E-cadherin staining was considered significant. EGFR scoring was performed on a scale of 0 to 3 as previously described(16): absence of membrane staining (0), incomplete staining in >10% of cells (1+), complete circumferential but weak membrane staining in >10% of cells (2+), and strong membrane staining in >10% of cells (3+). Nuclear p53 immunostaining was scored on the following semiquantitative scale as previously reported(17): no staining (0); focal to <10% of cells (1+); 10-50% of cells or weak staining in >50% of cells (2+); strong staining of >50% of cells (3+). p16 was graded as absent/weak (0), strong nuclear and cytoplasmic staining (1+), strong cytoplasmic reactivity (2+). A three tiered scale was used for p21 and p27: negative (0), focal staining in <50% of tumor nuclei, positive staining in (>50% of tumor nuclei).

FISH studies

Dual color FISH studies were performed either on tissue microarrays (n=29) or unstained microsections (n=4). In brief, 5 μ sections were baked overnight at 56°C and deparaffinized in Citrasolv (15 minutes × 2) followed by 100% ethanol for 10 minutes. Thereafter, the slides were placed in 10 mM citric acid (pH 6.08) and microwaved at the high setting for 3 minutes. This was followed by pepsin digestion (4mg Pepsin/L 0.9% NaCl) for 15 minutes in a 37°C waterbath and serial dehydration with increasing concentrations of ethanol. The following locus specific (LSI) probes were employed: *EGFR* (7p12), *P16* (9p21), *PTEN* (10q23) and *RB1* (13q14) (SpectrumOrange™, Abbott Molecular/Vysis, Des Plaines, IL) as well as *PDGFRA* (custom made; SpectrumGreen™) with respective reference probes (CEP 4 SpectrumOrange™; CEP 7, 9, 10, and LSI 13q34; SpectrumGreen™), codenatured with the tissue sections and hybridized overnight at 37°C. After hybridization the slides were

washed on 2XSSC/0.1%NP-40 for 2 minutes at 73°C, counterstained with DAPI and coverslipped. At least 100 tumor cells per case were enumerated by one of us (FJR) in each of the different tissue components using a Zeiss AxioPlan 2 fluorescent microscope and imaging system. Amplification and deletion were defined as a ratio of LSI to control probe of >2 or less than 0.8, respectively. Monosomy and chromosomal gain were defined as loss of the control probe in 60% of cells and gain in 30% of cells, respectively.

Statistical Methods

Patient and tumor characteristics were described with medians, interquartile ranges (IQR), ranges, and frequencies. Overall and recurrence-free survivals were evaluated using the Kaplan Meier method. Categorical variables were compared with the Fisher exact test. All tests were 2-sided with any p-value less than 0.05 considered statistically significant. Statistical analyses were performed with SAS software (SAS Institute Inc., Cary, NC).

Results

General

A total of 60 cases were found among approximately 3500 glioblastomas (1.7%) operated and/or reviewed at the Mayo Clinic, Rochester, MN from 1986-2007. After pathologic review, two cases of glioblastomas with PNET-like areas(18,19)were excluded because of the presence of proliferative nodules with neuropil and strong synaptophysin staining. The remaining cases were assigned to three different groups based upon the criteria outlined above: A-GBM (n=28)(48%), E-GBM (n=10)(17%), and TE-GBM (n=20)(35%). Material from recurrent tumor was available for review in 5 cases, in addition to the primary.

Original histopathologic diagnoses or preliminary interpretations prior to consultation, identified mostly from related correspondence, were available for 37 cases; these included high grade glioma/GBM (46%), metastatic carcinoma (16%), malignant neoplasm (11%), ependymoma (8%), glioneuronal tumor/PNET(8%), meningioma (5%), sarcoma (3%), and lymphoma (3%).

Clinical Features

Clinical and demographic features of the three tumor groups are summarized in table 1. There were 38 males and 20 females with a median age at diagnosis of 57 years (IQR, 50 to 67). A prior diagnosis of breast or prostatic adenocarcinoma had been made in 3 and 2 patients respectively. Postoperative treatment consisted of radiation therapy (n=11), radiation and chemotherapy (n=10), including Temodar (n=7) or BCNU (n=2), observation (n=3) or unknown (n=34).

Pathology

General—Relevant histologic features are summarized in table 2 and illustrated in figures 1-3. The glial component featured fibrillary astrocytes (n=46), gemistocytes (n=8), and multinucleated giant cells (n=5). Vascular changes took the form of endothelial hypertrophy or glomeruloid vasculature. No convincing “endothelial proliferation” (apparent multilayering of the endothelium) was noted in any case. Although necrosis was an almost universal finding in the primary tumors prior to radiation therapy, it was more often coagulative than pseudopalisading (84 vs 10%). In three cases where necrosis was not evident on the slides available for review, necrosis was documented either in the pathology report (n=2) or in the form of radiologic findings, consistent with necrosis (n=1). Microthrombi within vessels were noted in 56% of the cases. Mitotic indices by group

counted (per 10 HPF median, IQR) was 40.5 (20,52) in A-GBM, 14 (8,22) in E-GBM, and 25.5 (11,30) in TE-GBM (p=0.002)

A total of 25 tumors (43%) featured a sarcomatous component, which was slightly more frequent in TE-GBMs (55%), although this was not statistically significant (p=0.38). The morphology of the sarcomatous component was most often fibrosarcoma (n=16) or pleomorphic spindle cell sarcoma (n=8). Heterologous elements included bone and/or cartilage (n=4) and rhabdomyoblasts (n=3).

A-GBM—An accompanying mucoid matrix was noted in 50% of cases, a frequency higher that E-GBM and TE-GBM (0 and 20% respectively)(p=0.006)(Figure 1). Unusual features included a chordoid pattern (n=4), granular cells (n=3), vacuolated cells (n=2), stromal eosinophils (n=1), granular bodies (n=1), and a focal astroblastic pattern in the glial component (n=1).

E-GBM—Round cells without conspicuous processes were the characteristic feature (Figure 2). Unusual features included scattered giant cells (n=1) and a desmoplastic response outlining isolated tumor nests. One E-GBM featured prominent xanthic changes, similar to those reported by Rosenblum et al(11), and was originally misdiagnosed as probable metastatic renal cell carcinoma.

TE-GBM—True epithelial differentiation took the form of epithelial nests with supportive immunohistochemical confirmation (n=11)(Figure 3), definite squamous differentiation (n=6), and true glands (n=3). Unusual features included stromal eosinophils (n=2) and granular bodies (n=1).

Immunohistochemistry: glial and epithelial markers

The results of staining for glial and epithelial markers are summarized in table 3. All tumors, at least focally, expressed glial markers (GFAP and/or S100), including the adenoid or epithelioid component. In decreasing frequency, the following were expressed in the epithelial component of TE-GBM: EMA (94%), cytokeratin CAM 5.2 (89%), E-cadherin (82%), cytokeratin AE1/AE3 (80%), cytokeratin 7 (73%), pCEA (73%), cytokeratin 5/6 (36%), cytokeratin 20 (7%). Conversely, only cytokeratins AE1/AE3 and 7 were present at a substantial frequency in the glial components of A-GBM (62% and 43%) and TE-GBM (53 and 27%), respectively. EMA was present in the adenoid component of A-GBM in 59% and in almost half of those cases in a membranous or dot-like pattern (24%). Synaptophysin immunopositivity was essentially limited to A-GBM, where it was mostly a focal/partial finding (36 and 15% in the adenoid and glial components respectively).

Immunohistochemistry: MIB-1 labeling index

Median (IQR) MIB-1 labeling indices in the most proliferative regions were 48.9 (25.7, 60.0) in A-GBM, 19.7 (16.2, 38.9) in E-GBM, and 36.2 (30.4, 44.4) in TE-GBM. In general median MIB-1 labeling indices were higher in the adenoid/epithelial than in the glial components of the A-GBM and TE-GBM groups combined [41.4 (11.3, 74.5) vs. 13.7 (6.6, 58.0) ($p<0.0001$)].

Molecular abnormalities identified by FISH and immunohistochemistry

The various molecular abnormalities are summarized by tumor group in table 4. Representative cases are illustrated in figure 4. Molecular cytogenetic abnormalities were identified in both the adenoid/ true epithelial and glial components in 54% of the cases; no abnormality predominated in one component versus the other, although *PDGFRA* amplification was present only in the glial component of two cases (7%). There was a trend

toward *RB1* deletion/-13q being more frequent in A-GBM (50%) vs the combined E-GBM and TE-GBM groups (11%)(p=0.06).

Stains for p21 were more frequently immunonegative in TE-GBM (93%) than in A-GBM (60%) and E-GBM (25%)(p=0.008). Both *EGFR* amplification and an EGFR immunohistochemical score of 3+ were more frequent in E-GBM (50 and 63%), than the other two groups combined (20 and 20% respectively), although only EGFR IHC reached statistical significance (p=0.03). A decrease in p27 expression was noted in cases with an associated sarcomatous component (gliosarcoma)(p=0.009). Immunostaining for p16 was negative/weak in 33%, but negative in all cases in which homozygous deletion was identified by FISH, in 2 (of 4) cases with heterozygous deletion, and in 1 (of 5) tumors with monosomy 9.

Survival analyses

Median overall and recurrence-free survival for the entire study group was 7 and 6 months after diagnosis (IQR 4 to 11 and 3 to 10 respectively), and did not differ significantly among the three tumor subgroups (figure 5). Furthermore, we found no significant associations with either overall or recurrence free survival and patient age, tumor size, lesion location, mitotic activity, the MIB-1 labeling index, or with molecular abnormalities detected by FISH or immunohistochemistry (p>0.05).

Discussion

The rare presence of epithelial-like or true epithelial elements, with or without sarcomatous metaplasia, may confound the diagnosis of infiltrating astrocytomas. The presence of compact, cohesive elements within gliosarcomas was first recognized and illustrated by Rubinstein in his classic manuscript on gliosarcomas(20). However, the first comprehensive description of so-called “adenoid glioblastoma” was provided by Kepes in a detailed clinicopathologic study of 5 cases, all of which had a sarcomatous component(7). Two related publications followed. One described papillary elements in adenoid glioblastoma, sometimes mimicking similar structures in medulloepithelioma(8). The other was a report of 6 glioblastomas with true epithelial differentiation, usually in the form of squamous nests, by the same authors(14).

The main differential diagnosis of the tumors in question is metastatic carcinoma. It should be emphasized that conventional astrocytomas are frequently labeled by a variety of cytokeratins, CAM 5.2 being of greatest utility in differentiating metastatic carcinoma from gliomas(21). This was confirmed in our study wherein the glial component was positive for CAM 5.2 in only a single case of TE-GBM. In such cases, the recognition of a malignant glial component is essential to the diagnosis, the caveat being that carcinoma metastatic to glioma has been reported(22,23). In that this usually occurs in the context of widespread metastatic disease, knowledge of the clinical history and perhaps morphologic comparison with the primary carcinoma is of importance. Five of our patients, three with TE-GBMs, had a prior history of breast or prostate carcinoma. In 3 of the 5 cases areas of transition from well differentiated astrocytes to small poorly differentiated cells to nests exhibiting frank epithelial differentiation were more consistent with epithelial metaplasia in glioma. In one instance, the metastatic work-up included whole body PET and CT scans, as well as bone scans; all failed to disclose metastatic disease. In cases of A-GBM, histologic transition as well as the presence of partial GFAP immunoreactivity in adenoid areas (88% of our cases) supports our diagnosis.

Aside from metastatic carcinoma other primary tumors enter into the differential diagnosis. These include ependymoma, choroid plexus carcinoma, medulloepithelioma,

craniopharyngioma, pituitary adenoma, and meningioma, especially the papillary subtype, and germ cell tumor. Three of our cases demonstrated gland-like cellular arrangements easily mistaken for ependymal true rosettes. Lack of perivascular pseudorosettes, the presence of an infiltrative astrocytic component, immunoreactivity for pCEA (a feature in two of the three cases), as well as a specific cytokeratin profile simplifies the distinction. Immunoreactivity for CEA is not a feature of ependymoma(24).

Also entering into the differential diagnosis of A-GBM is what has been recently termed "GBM with PNET-like/neuroblastic areas"(18,19). Although our study excluded tumors with overt neuronal differentiation, admitting only lesions with cohesive cell nests resembling epithelial structures, it is of note that 43% of the A-GBM tested were positive for synaptophysin (partial/weak in all but one). This in addition to the general high proliferative activity of the adenoid component as compared to the glial component, suggests a possible relationship between some A-GBM and the GBM-PNET alluded above.

Yet another rare glioblastoma variant characterized by cohesive epithelial-appearing cells exhibiting varying degrees of lipidization was reported by Rosenblum et al(11). An additional 6 probable cases were reported in abstract form(25), and three as part of a series of glioblastomas affecting young adults(12). Their main differential diagnosis in these tumors is again metastatic carcinoma as well as melanoma.

Although there have been a few reports of A-GBM/TE-GBM focusing on their clinicopathologic features, publications regarding their molecular genetic characteristics are scarce. Loss of heterozygosity (LOH) studies utilizing polymorphic microsatelite markers in various components of one TE-GBM reported by Ozolek et al. supported their monoclonal origin(15). The losses corresponded to regions 1p36, *p16* (9p21), *PTEN* (10q23) and *TP53* (17p13), regions commonly affected in high grade astrocytomas. Similarly, Du Plessis et al(13) found an identical truncating *TP53* mutation as well as LOH at 17p13 and 10q22-26 in both components of a TE-GBM. Lastly, Mueller et al. demonstrated identical *TP53* mutations in both components of 2 of 5 glioblastomas with epithelial/adenoid morphology(26).

The present study employed interphase cytogenetics (FISH) to assess alterations previously studied in conventional gliomas by traditional cytogenetics or, more recently, by high throughput techniques including single nucleotide polymorphism analysis coupled to novel statistical algorithms (27). *P16* deletion/monosomy 9 was our most common finding, being present in 65% of our cases. By comparison, in primary glioblastoma, *p16* deletion occurs in one third of the cases (28,29). Both *EGFR* amplification and overexpression seemed more frequent in E-GBM (50 and 63%) than in A-GBM or TE-GBM, a frequency similar to that noted in conventional primary glioblastoma, wherein *EGFR* amplification is present in approximately 40% of tumors(29). The fact that *EGFR* amplification is rare in gliosarcomas(30,31) might partially explain our findings, in that a sarcomatous component was more frequent in A-GBM and TE-GBM.

Adenoid-GBM had a higher frequency of *RB1* deletions/-13q (50%) than did other tumor groups. A similar frequency of 13q LOH has been reported to occur in one third to one half of astrocytomas(32). Other mechanisms, including promoter methylation of *RB1* are also frequent in glioblastomas, although they may be more common in secondary GBM(33). *RB1* promoter hypermethylation may occur in the absence of LOH in some GBMs and may in itself explain the inactivation of this important tumor suppressor gene. Further similarities to conventional glioblastoma included frequent monosomy 10/*PTEN* deletion in all subgroups in our study (63%).

It is of note that molecular cytogenetic imbalances were identified in both tumor components in 54% of the cases. This compares favorably with the study on gliosarcomas by Actor et al, who found a 57% frequency of allelic imbalances to be present in both components on comparative genomic hybridization(30). Similar results were reported in a smaller FISH study by Paulus and colleagues(34). These results may be explained in part by tumor heterogeneity, as well as by an admixture of non-neoplastic cells.

Although we did not find any prognostic differences with respect to immunostaining for cell cycle regulators, several interesting patterns emerged, with decrease in p21 and increased p53 staining in TE-GBM. p27 loss was also associated with the presence of a sarcomatous component. The latter finding is relevant since some authors have found an association with p27 loss and high grade in oligodendrogliomas(35), as well as survival in high grade astrocytomas(36).

It is of note that although survival was on average poor for all groups, the patients received heterogeneous treatment approaches, given the necessary retrospective nature of this study of a rare glioblastoma variant. In the past several years the standard of treatment for patients with glioblastoma has changed given the survival benefit provided by temozolamide chemotherapy (37). Therefore, our results with respect to survival should be interpreted with caution.

In summary, our study sought to explore the pathologic, immunophenotypic and a subset of molecular characteristics of glioblastomas with various degrees of epithelial morphology. The molecular abnormalities of these tumors overlap with those of conventional glioblastomas and gliosarcomas, although they do seem to vary by tumor subgroup. It is essential for diagnosticians to be aware of these tumors in order to avoid extensive, unnecessary searches for a primary neoplasm elsewhere. Further studies are also needed to explore additional pathobiologic and prognostic differences associated with these enigmatic morphologies.

Acknowledgments

The authors would like to thank the clinicians and pathologists who provided follow-up information, as well as the Cytogenetic and the Tissue and Cell Molecular Analysis (TACMA) shared resources of the Mayo Clinic Cancer Center for technical assistance.

This work was supported in part by NIH training grant T32 NS07494-04 (FJR)

References

1. Louis, D.; Ohgaki, H.; Wiestler, O.; Cavenee, W. WHO Classification of Tumours of the Central Nervous System. 4th ed. IARC press; Lyon, France: 2007.
2. Banerjee AK, Sharma BS, Kak VK, Ghatak NR. Gliosarcoma with cartilage formation. Cancer. 1989; 63(3):518–523. [PubMed: 2643455]
3. Hayashi K, Ohara N, Jeon HJ, et al. Gliosarcoma with features of chondroblastic osteosarcoma. Cancer. 1993; 72(3):850–855. [PubMed: 8334639]
4. Barnard RO, Bradford R, Scott T, Thomas DG. Gliomyosarcoma. Report of a case of rhabdomyosarcoma arising in a malignant glioma. Acta Neuropathologica. 1986; 69(1-2):23–27. [PubMed: 3962596]
5. Haddad SF, Moore SA, Schelper RL, Goeken JA. Smooth muscle can comprise the sarcomatous component of gliosarcomas. J Neuropathol Exp Neurol. 1992; 51(5):493–498. [PubMed: 1381414]
6. Vlodavsky E, Konstantinesku M, Soustiel JF. Gliosarcoma with liposarcomatous differentiation: the new member of the lipid-containing brain tumors family. Archives of Pathology & Laboratory Medicine. 2006; 130(3):381–384. [PubMed: 16519569]

7. Kepes JJ, Fulling KH, Garcia JH. The clinical significance of “adenoid” formations of neoplastic astrocytes, imitating metastatic carcinoma, in gliosarcomas. A review of five cases. Clin Neuropathol. 1982; 1(4):139–150. [PubMed: 6188569]
8. Mork SJ, Rubinstein LJ, Kepes JJ. Patterns of epithelial metaplasia in malignant gliomas. I. Papillary formations mimicking medulloepithelioma. J Neuropathol Exp Neurol. 1988; 47(2):93–100. [PubMed: 2828555]
9. Akimoto J, Namatame H, Haraoka J, Kudo M. Epithelioid glioblastoma: a case report. Brain Tumor Pathol. 2005; 22(1):21–27. [PubMed: 18095100]
10. Shintaku M, Hirano A, Llena JF. [Fine structure of glioblastoma multiforme with “adenoid formation”]. No Shinkei Geka. 1988; 16(8):997–1003. [PubMed: 2845290]
11. Rosenblum MK, Erlandson RA, Budzilovich GN. The lipid-rich epithelioid glioblastoma. Am J Surg Pathol. 1991; 15(10):925–934. [PubMed: 1718177]
12. Kleinschmidt-DeMasters BK, Meltesen L, McGavran L, Lillehei KO. Characterization of glioblastomas in young adults. Brain Pathol. 2006; 16(4):273–286. [PubMed: 17107596]
13. du Plessis DG, Rutherfoord GS, Joyce KA, Walker C. Phenotypic and genotypic characterization of glioblastoma multiforme with epithelial differentiation and adenoid formations. Clin Neuropathol. 2004; 23(4):141–148. [PubMed: 15328877]
14. Mork SJ, Rubinstein LJ, Kepes JJ, Perentes E, Uphoff DF. Patterns of epithelial metaplasia in malignant gliomas. II. Squamous differentiation of epithelial-like formations in gliosarcomas and glioblastomas. J Neuropathol Exp Neurol. 1988; 47(2):101–118. [PubMed: 3339369]
15. Ozolek JA, Finkelstein SD, Couce ME. Gliosarcoma with epithelial differentiation: immunohistochemical and molecular characterization. A case report and review of the literature. Mod Pathol. 2004; 17(6):739–745. [PubMed: 15148503]
16. Layfield LJ, Willmore C, Tripp S, Jones C, Jensen RL. Epidermal growth factor receptor gene amplification and protein expression in glioblastoma multiforme: prognostic significance and relationship to other prognostic factors. Appl Immunohistochem Mol Morphol. 2006; 14(1):91–96. [PubMed: 16540738]
17. Giannini C, Hebrink D, Scheithauer BW, Dei Tos AP, James CD. Analysis of p53 mutation and expression in pleomorphic xanthoastrocytoma. Neurogenetics. 2001; 3(3):159–162. [PubMed: 11523567]
18. Perry A, Miller CR, Gujrati M, et al. Malignant Gliomas with Primitive Neuroectodermal Tumor-like Components: A Clinicopathologic and Genetic Study of 53 Cases. Brain Pathol. Apr 29.2008 [Epub ahead of print].
19. Wharton SB, Whittle IR, Collie DA, Bell HS, Ironside JW. Gliosarcoma with areas of primitive neuroepithelial differentiation and extracranial metastasis. Clin Neuropathol. 2001; 20(5):212–218. [PubMed: 11594506]
20. Rubinstein LJ. The development of contiguous sarcomatous and gliomatous tissue in intracranial tumours. J Pathol Bacteriol. 1956; 71(2):441–459. [PubMed: 13398890]
21. Oh D, Prayson RA. Evaluation of epithelial and keratin markers in glioblastoma multiforme: an immunohistochemical study. Arch Pathol Lab Med. 1999; 123(10):917–920. [PubMed: 10506444]
22. Muller W, Schroder R. Spreading of metastases into cranial tumors: metastasis of a breast carcinoma to a pilocytic astrocytoma. Clin Neuropathol. 1999; 18(3):109–112. [PubMed: 10361994]
23. Mork SJ, Rubinstein LJ. Metastatic carcinoma to glioma: a report of three cases with a critical review of the literature. J Neurol Neurosurg Psychiatry. 1988; 51(2):256–259. [PubMed: 2831305]
24. Vege KD, Giannini C, Scheithauer BW. The immunophenotype of ependymomas. Appl Immunohistochem Mol Morphol. 2000; 8(1):25–31. [PubMed: 10937045]
25. Fuller GN, Goodman JC, Vogel H, Ghorbani R. Epithelioid glioblastoma: a distinct clinicopathologic entity (abstract). J Neuropathol Exp Neurol. 1998; 57:501.
26. Mueller W, Lass U, Herms J, Kuchelmeister K, Bergmann M, von Deimling A. Clonal analysis in glioblastoma with epithelial differentiation. Brain Pathol. 2001; 11(1):39–43. [PubMed: 11145202]

27. Beroukhim R, Getz G, Nghiemphu L, et al. Assessing the significance of chromosomal aberrations in cancer: methodology and application to glioma. Proc Natl Acad Sci U S A. 2007; 104(50): 20007–20012. [PubMed: 18077431]

28. Biernat W, Tohma Y, Yonekawa Y, Kleihues P, Ohgaki H. Alterations of cell cycle regulatory genes in primary (de novo) and secondary glioblastomas. Acta Neuropathol. 1997; 94(4):303–309. [PubMed: 9341929]

29. Ohgaki H, Kleihues P. Genetic pathways to primary and secondary glioblastoma. Am J Pathol. 2007; 170(5):1445–1453. [PubMed: 17456751]

30. Actor B, Cobbers JM, Buschges R, et al. Comprehensive analysis of genomic alterations in gliosarcoma and its two tissue components. Genes Chromosomes Cancer. 2002; 34(4):416–427. [PubMed: 12112531]

31. Reis RM, Konu-Leblebicioglu D, Lopes JM, Kleihues P, Ohgaki H. Genetic profile of gliosarcomas. Am J Pathol. 2000; 156(2):425–432. [PubMed: 10666371]

32. Henson JW, Schnitker BL, Correa KM, et al. The retinoblastoma gene is involved in malignant progression of astrocytomas. Ann Neurol. 1994; 36(5):714–721. [PubMed: 7979217]

33. Nakamura M, Yonekawa Y, Kleihues P, Ohgaki H. Promoter hypermethylation of the RB1 gene in glioblastomas. Lab Invest. 2001; 81(1):77–82. [PubMed: 11204276]

34. Paulus W, Bayas A, Ott G, Roggendorf W. Interphase cytogenetics of glioblastoma and gliosarcoma. Acta Neuropathol (Berl). 1994; 88(5):420–425. [PubMed: 7847070]

35. Korshunov A, Golanov A. The prognostic significance of DNA topoisomerase II-alpha (Ki-S1), p21/Cip-1, and p27/Kip-1 protein immunoexpression in oligodendrogliomas. Arch Pathol Lab Med. 2001; 125(7):892–898. [PubMed: 11419973]

36. Kirla RM, Haapasalo HK, Kalimo H, Salminen EK. Low expression of p27 indicates a poor prognosis in patients with high-grade astrocytomas. Cancer. 2003; 97(3):644–648. [PubMed: 12548606]

37. Stupp R, Mason WP, van den Bent MJ, et al. Radiotherapy plus concomitant and adjuvant temozolomide for glioblastoma. N Engl J Med. 2005; 352:987–96. [PubMed: 15758009]

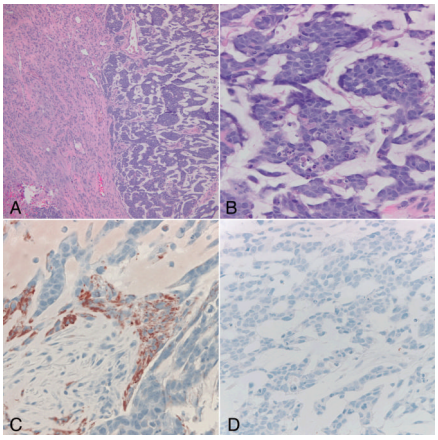

Figure 1.

Case 34. Adenoid glioblastoma demonstrating sharply demarcated areas of infiltrative astrocytoma (left) juxtaposed to cords and gland-like structures in a myxoid background (right)(A)(H&Ex 100). High power view of the adenoid component demonstrates cohesive hyperchromatic cells with frequent mitoses and apoptotic bodies (B)(H&Ex 400). Immunohistochemical stains demonstrate immunoreactivity for GFAP (C) and absence of synaptophysin (D) in the adenoid component (x400).

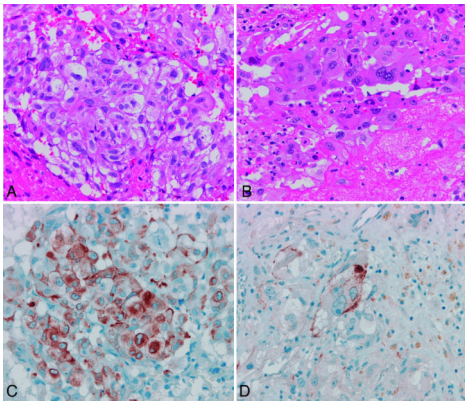

Figure 2.

Case 42. Glioblastoma with epithelioid and true epithelial differentiation. The tumor was largely composed of epithelioid cells with scant processes (A) with focal areas where cells acquired more eosinophilic cytoplasm and prominent nucleoli (B)(H&Ex 400). GFAP (C) and CAM 5.2 (D) immunoreactivity were present in the former and latter areas respectively (x 400).

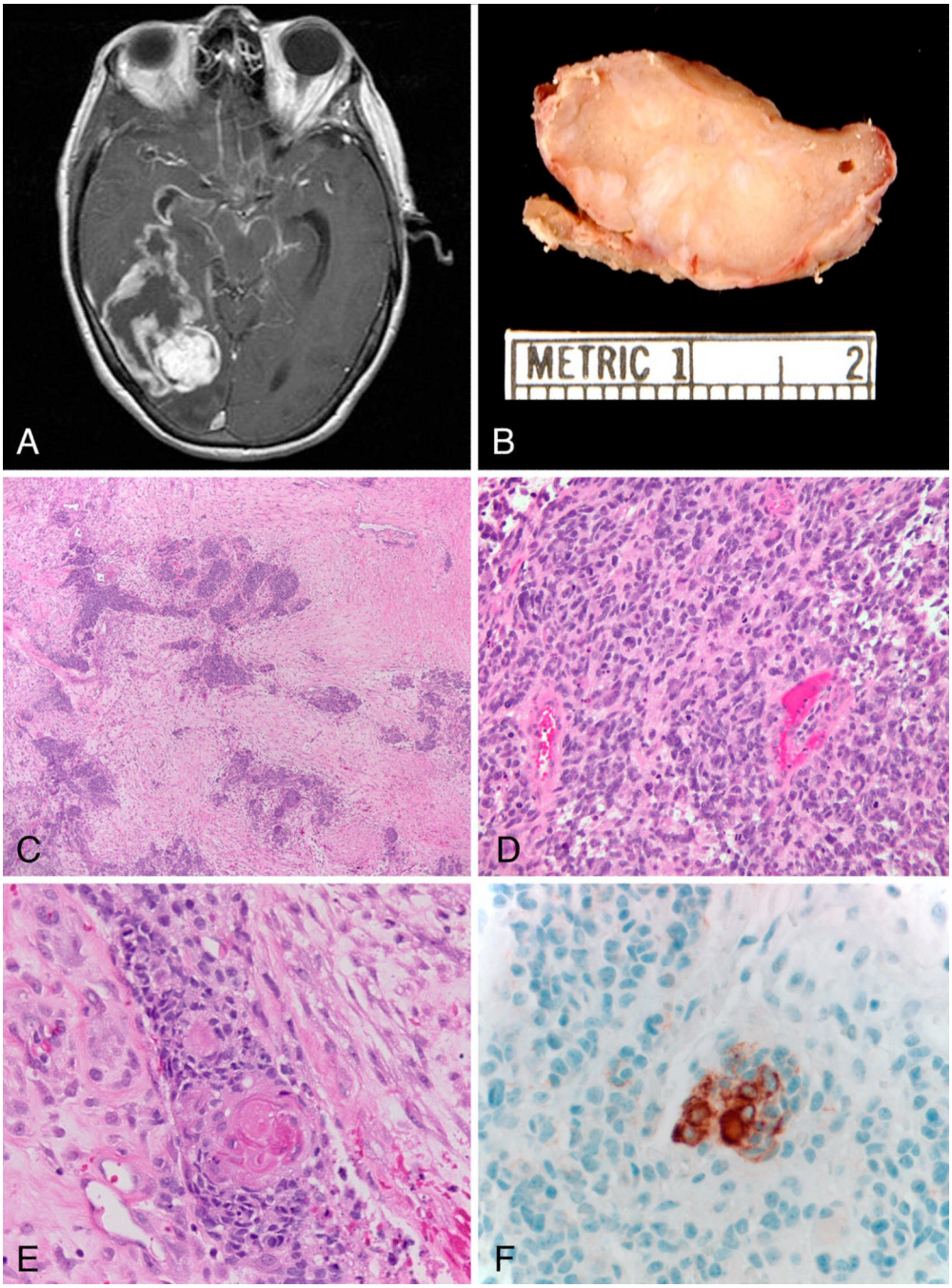

Figure 3.

Case 46. Glioblastoma with true epithelial differentiation. T1-weighted axial MRI post-contrast demonstrates a large mass with ring-enhancement occupying a large portion of the right temporal lobe(A). Gross photo of a section in a solid area of the tumor demonstrates a firm tan mass with white streaks, reflecting desmoplasia. A portion of overlying meninges is also present at the bottom of the figure (B). Low power view highlighting cohesive nests in a desmoplastic stroma (C)(H&Ex 40). Infiltrative glial component (D)(H&Ex 200). Several tumor nests contained tight keratin pearls consistent with true epithelial differentiation (E) (H&Ex 400). The keratin pearls were immunoreactive with cytokeratin CAM 5.2 (F)(x400).

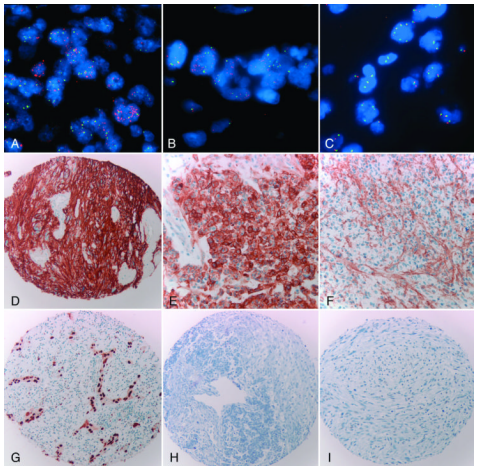

Figure 4.

Abnormalities of EGFR and cell cycle inhibitors. Dual color FISH studies (A-C) and immunohistochemical stain for EGFR (D-F). EGFR amplification and overexpression were frequent in E-GBM (A,D). *EGFR* amplification was a focal finding in one case of TE-GBM, being present in the adenoid/epithelial (B) but not the glial (C) component. Immunohistochemistry was patchy in this case, with strong overexpression of EGFR in some “adenoid/epithelial” fields (E) but not in others (F). Epithelial component of a TE-GBM demonstrating strong immunoreactivity for p53 (G). Loss of p21 immunoreactivity in the epithelial and glial components of a TE-GBM (H). Loss of p27 expression in the glial and sarcomatous components of a gliosarcoma (I).

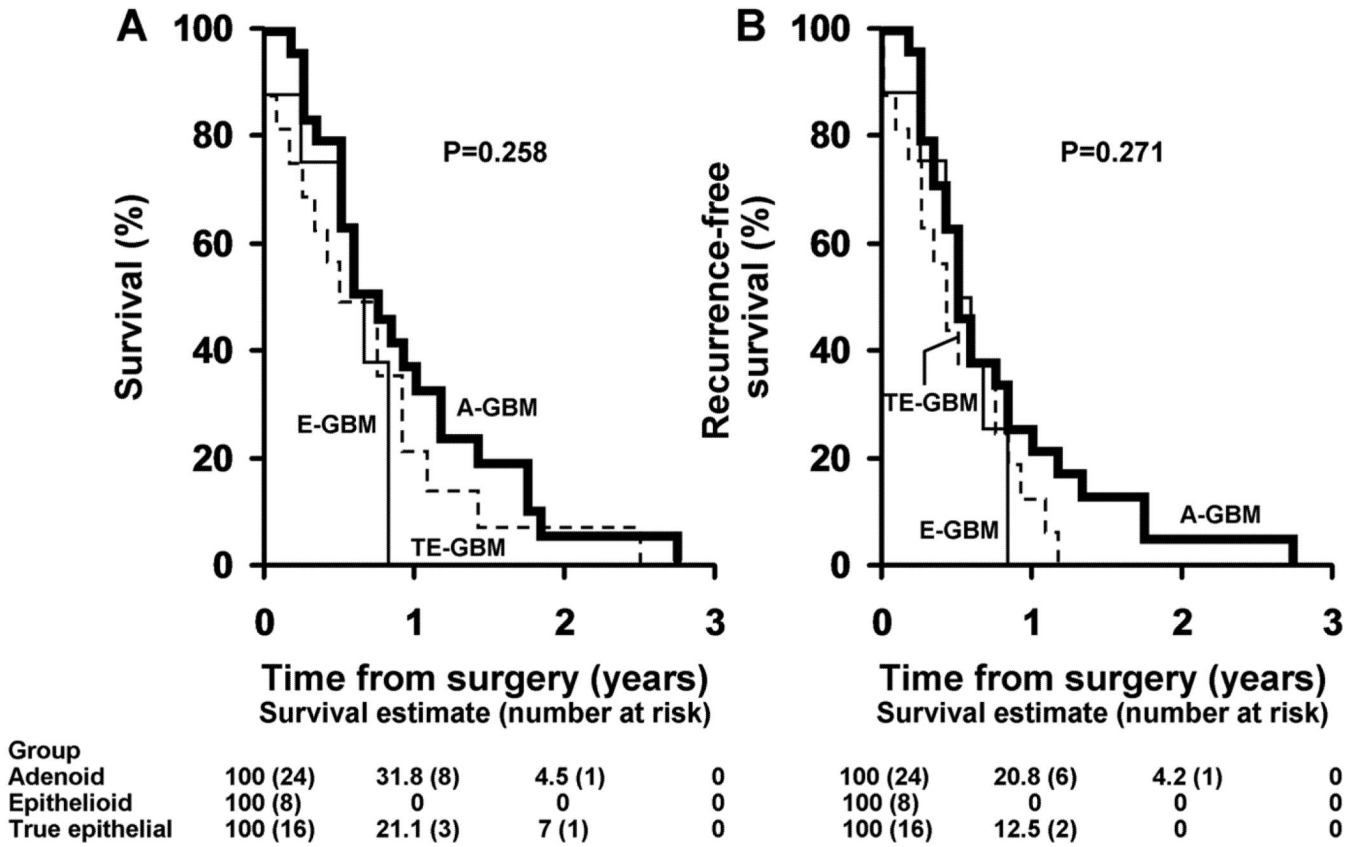

Figure 5.

Overall and recurrence free survival in adenoid (A-GBM), true epithelial (TE-GBM) and epithelioid (E-GBM) glioblastomas. Kaplan-Meier plots demonstrate poor overall (A) and recurrence-free (B) survival for all groups. Survival was not statistically different between the subgroups.

Table 1

Demographic and Clinical Data of adenoid (A-GBM), true epithelial (TE-GBM) and Epithelioid (E-GBM) glioblastomas

	A-GBM	E-GBM	TE-GBM
Frequency n(%)	28 (48)	10 (17)	20 (35)
Age in years (median,IQR)	57 (50, 67)	53 (44, 63)	56(51, 71)
Gender (M:F)	20:8	5:5	13:7
Location n(%)			
Temporal lobe	11 (44)	1 (11)	8 (40)
Frontal lobe	2 (8)	1(11)	5 (25)
Parietal lobe	4 (16)	3 (33)	1 (5)
Occipital lobe	1 (4)	0 (0)	0 (0)
Two lobes	5 (20)	2 (22)	4 (20)
Cerebellum	2 (8)	0 (0)	0 (0)
Spinal cord	0 (0)	0 (0)	1 (5)
Lateral ventricle	0 (0)	2 (22)	1 (5)
Size in cm (median, IQR)	4 (3.5-6.2)	4.7(3.5-5.5)	5 (2.5-5.5)
[1]Imaging Features n(%)			
Heterogeneous enhancement	3 (33)	6 (67)	5 (42)
Ring-enhancement	5 (56)	1 (11)	7 (58)
Leptomeningeal enhancement	1 (11)	0 (0)	1 (8)
Circumscribed	2 (22)	0 (0)	0 (0)
Cystic component	1 (11)	2 (22)	2 (17)
Satellite lesions	4 (44)	0 (0)	1 (8)

[1]-radiologic data was available in 9 (of 28) A-GBM (32%), 9 (of 10) E-GBM (90%) and 12 (of 20) TE-GBM (60%).

Table 2

Pathologic features by group in adenoid (A-GBM), true epithelial (TE-GBM) and Epithelioid (E-GBM) glioblastomas

N(%) present	A-GBM	E-GBM	TE-GBM
Frequency	28 (48)	10 (17)	20 (35)
Sarcomatous component	11 (39)	3 (30)	11 (55)
Papillary structures	6 (21)	1 (10)	6 (30)
Whorls	6 (21)	1 (10)	10 (50)
Myxoid Stroma	14 (50)	0 (0)	4 (20)
Vascular changes	12 (43)	6 (60)	10 (50)
Hypertrophy	8 (29)	5 (50)	7 (35)
Glomeuroloid vessels	4 (14)	1 (10)	2 (20)
Necrosis			
Pseudopalisading	2 (7)	1(10)	3 (15)
Coagulative	24(86)	9 (90)	16 (80)
Inflammation	8 (29)	1 (10)	5 (25)
Hemosiderin	9 (32)	5 (50)	5 (25)
Most proliferative component			
Adenoid/epithelial	25 (96)	2 (20)	16 (84)
Glial	1 (4)	7 (70)	2 (11)
Sarcoma	0 (0)	1 (10)	1 (5)
Evident Infiltrative glial component			
At diagnosis	17 (61)	6 (60)	11 (61)
At recurrence	1 (4)	1 (10)	1 (6)

Table 3

Immunohistochemical features of glial and epithelial markers in different tissue components of adenoid (A-GBM), true epithelial (TE-GBM) and epithelioid (E-GBM) glioblastomas

	A-GBM		E-GBM	TE-GBM	
Component n (% of evaluable cases)	***Glial***	***Adenoid***		***Glial Epithelial***	
GFAP					
Negative	0 (0)	3 (12)	0 (0)	0 (0)	3 (16)
Focal	4 (17)	19 (76)	3 (30)	3 (16)	14 (74)
Partial/Moderate	7 (30)	2 (8)	3 (30)	6 (32)	1 (5)
strong	12 (52)	1 (4)	4 (40)	10 (53)	1 (5)
S100					
Negative	0 (0)	0 (0)	1 (20)	0 (0)	1 (8)
Focal	0 (0)	6 (35)	1 (20)	1 (7)	5 (38)
Partial/Moderate	4 (27)	6 (35)	0 (0)	3 (20)	5 (38)
strong	11 (73)	5 (29)	3 (60)	11 (73)	2 (15)
CK AE1/AE3					
Negative	5 (38)	10 (77)	4 (67)	7 (47)	3 (20)
Partial	4 (31)	2 (15)	1 (17)	5 (33)	5 (33)
Positive	4 (31)	1 (8)	1 (17)	3 (20)	7 (47)
CK CAM 5.2					
Negative	20 (100)	21 (100)	9 (100)	19 (95)	2 (11)
Partial	0 (0)	0 (0)	0 (0)	1 (5)	6 (32)
Positive	0 (0)	0 (0)	0(0)	0 (0)	11 (58)
CK 5/6					
Negative	8 (100)	7 (88)	6 (100)	12 (100)	7 (64)
Partial	0 (0)	1 (12)	0(0)	0 (0)	2 (18)
Positive	0 (0)	0 (0)	0(0)	0 (0)	2 (18)
CK 7					
Negative	8 (57)	11 (69)	4 (57)	11 (73)	4 (27)
Partial	4 (29)	4 (25)	1 (14)	2 (13)	4 (27)
Positive	2 (14)	1 (6)	2 (29)	2 (13)	7 (47)
CK 20					
Negative	14 (100)	16 (100)	7 (100)	15 (100)	13 (93)
Partial	0 (0)	0 (0)	0 (0)	0 (0)	1 (7)
Positive	0 (0)	0 (0)	0 (0)	0 (0)	0 (0)
EMA					
Negative	13 (76)	7 (41)	3 (33)	14 (82)	1 (6)
Focal	2 (12)	4 (24)	1 (11)	1 (6)	2 (13)
Membranous/dots	0 (0)	4 (24)	4 (44)	1 (6)	13 (81)
Cytoplasmic	2 (12)	2 (12)	1 (11)	1 (6)	0 (0)
pCEA					
Negative	14 (100)	13 (93)	5 (100)	16 (100)	4 (27)

	A-GBM		E-GBM	TE-GBM	
Component n (% of evaluable cases)	***Glial***	***Adenoid***		***Glial Epithelial***	
Partial	0 (0)	0 (0)	0 (0)	0 (0)	6 (40)
Positive	0 (0)	1 (7)	0 (0)	0 (0)	5 (33)
E-cadherin					
Negative	9 (90)	5 (56)	2 (67)	11 (79)	2 (18)
Membranous	1 (10)	3 (33)	1 (33)	3 (21)	8 (73)
Membranous+cytoplasmic	0 (0)	1 (11)	0 (0)	0 (0)	1 (9)
Beta catenin					
Negative	1 (11)	0 (0)	0 (0)	3 (21)	0 (0)
Membranous	4 (44)	7 (64)	2 (67)	3 (21)	6 (46)
Membranous+cytoplasmic	4 (44)	4 (36)	1 (33)	8 (57)	7 (54)
Synaptophysin					
Negative	10 (77)	8 (57)	8 (100)	12 (92)	11 (92)
Partial	2 (15)	5 (36)	0 (0)	1 (8)	1 (8)
Positive	1 (8)	1 (7)	0 (0)	0 (0)	0 (0)
Chromogranin					
Negative	8 (100)	8 (100)	4 (100)	10 (83)	9 (82)
Partial	0 (0)	0 (0)	0 (0)	2 (17)	2 (18)
Positive	0 (0)	0 (0)	0(0)	0(0)	0 (0)
TTF-1					
Negative	10 (100)	8 (89)	4 (100)	13 (100)	12 (100)
Weakly positive	0 (0)	1 (11)	0 (0)	0 (0)	0 (0)
CDX-2					
Negative	6 (100)	6 (100)	4 (100)	10 (100)	9 (100)
INI-1					
Positive	3 (100)		8 (100)	1 (100)	

Table 4

Molecular abnormalities identified by FISH and/or Immunohistochemistry in adenoid (A-GBM), Epithelioid (E-GBM) and true epithelial (TE-GBM) glioblastomas as well as tumors that showed a sarcomatous component (GS).

N (%)	A-GBM	E-GBM	TE-GBM	TOTAL	GS
P16 deletion/−9	6 (60)	5 (71)	9 (64)	20 (65)	11 (73)
−10	4 (40)	5 (63)	8 (57)	17 (54)	8 (53)
PTEN deletion	1 (10)	2 (25)	4 (29)	7 (22)	2 (13)
EGFR amplification	1 (10)	4 (50)	4 (27)	9 (27)	2 (13)
+7	7 (70)	3 (38)	6 (40)	16 (48)	9 (60)
RB1 deletion/−13q	5 (50)	0 (0)	2 (14)	7 (25)	4 (31)
PDGFRA amplification	1 (10)	1 (25)	0 (0)	2 (7)	1 (8)
P53 IHC (3+)	4 (29)	2 (29)	7 (41)	13 (34)	6 (35)
P16 IHC					
Negative/weak	4 (31)	4 (67)	4 (24)	12 (33)	7 (41)
Cytoplasmic only	0 (0)	1 (17)	2 (12)	3 (8)	2 (12)
P21 IHC					
Negative	6 (60)	1 (25)	13 (93)	20 (71)	11 (85)
P27 IHC					
Negative	2 (20)	1 (33)	3 (23)	6 (23)	2 (15)
Focal	6 (60)	1 (33)	8 (62)	15 (58)	11 (85)
Positive	2 (20)	1 (33)	2 (15)	5 (19)	0 (0)
EGFR IHC (3+)	3 (21)	5 (63)	3 (19)	11 (29)	3 (18)

IHC=immunohistochemistry